

Research Article

Stability of Phenobarbital *N*-Glucosides: Identification of Hydrolysis Products and Kinetics of Decomposition

Floyd B. Vest,¹ William H. Soine,^{1,2} Richard B. Westkaemper,¹ and Phyllis J. Soine³

Received August 15, 1988; accepted January 25, 1989

The two diastereomers of 1-(1- β -D-glucopyranosyl)phenobarbital, (1A) and (1B), decompose to 1-(1- β -D-glucopyranosyl)-3-(2-ethyl-2-phenylmalonyl)urea (2A or 2B) followed by decarboxylation to 1-(1- β -D-glucopyranosyl)-3-(2-phenylbutyryl)urea (3A and 3B) under physiological conditions of temperature and pH. The sigmoidal pH-rate profile and the Arrhenius parameters indicate that degradation takes place by hydroxide ion attack on the undissociated and monoanion forms of 1A and 1B. The rates of hydrolysis of the nonionized species of 1A and 1B are more than two orders of magnitude faster than those of common 5,5-disubstituted or 1,5,5-trisubstituted barbiturates. Molecular modeling studies suggest that rate enhancement is due to intramolecular hydrogen bonding in the transition state of the C₂' hydroxyl with the tetrahedral hydrated C₆ carbonyl as well as hindered rotation around the N₁-C₁' of phenobarbital and glucose. Based on these studies it is recommended that any data related to the quantitation of 1A and 1B be reevaluated depending on how the samples were collected, stored, and analyzed.

KEY WORDS: phenobarbital *N*-glucosides; 1-(1- β -D-glucopyranosyl)-3-(2-phenylbutyryl)urea; hydrolysis; thermodynamics; molecular modeling.

INTRODUCTION

In man *N*-glucosylation has proven to be a quantitatively significant route of metabolism for amobarbital and phenobarbital (PB) following oral administration (1-8). During the development of a high-performance liquid chromatographic (HPLC) method for quantitating the two diastereomers of 1-(1- β -D-glucopyranosyl)phenobarbital (1A and 1B) (Fig. 1), it was observed that in samples stored for analysis, both *N*-glucoside conjugates underwent decomposition under conditions in which no decomposition of phenobarbital was detected. The conditions suggested that these metabolites were much more unstable than previously anticipated. To continue studies with these novel metabolites it was necessary to investigate the conditions under which these metabolites decomposed in order to minimize this problem. This report describes the identification of the initial decomposition products, the kinetics of the decomposition, and a proposed mechanism consistent with these observations.

MATERIALS AND METHODS

Reagents and Chemicals

Compounds 1A and 1B were synthesized as previously

described (9); in that report they were designated PBGA and PBGB, respectively. Since the absolute configuration of 1A and 1B is currently unknown, the naming is an arbitrary designation based on HPLC retention times, with 1A being the early-eluting peak and 1B the later-eluting peak. Phenylethylmalonamide (PEM) was obtained from Aldrich Chemical Co. (Milwaukee, Wis.) and was used as an analytical standard and for spectroscopic comparisons. All other solvents and chemicals were of analytical reagent grade or HPLC grade.

Equipment

Melting points (uncorrected) were determined in an open capillary with a Thomas-Hoover Unimelt apparatus (Philadelphia, Pa.). IR spectra were determined with a Nicolet 5ZDX FT-IR (Madison, Wis.). ¹H-NMR spectra were obtained on a JEOL FX90Q spectrometer (Tokyo, Japan). Optical rotations were determined on a Perkin-Elmer 141 Polarimeter (Norwalk, Conn.). All constant temperature incubations were done using a Thermajust Heating Block ($\pm 0.5^\circ\text{C}$, TechniLab Instrument, Pequannock, N.J.). UV analyses were obtained with a Varian DMS 100S UV/visible spectrophotometer (Palo Alto, Calif.) at a slit width of 1.0 nm.

Molecular mechanics calculations and graphic manipulations were performed using the CHEM-X system (Chemical Designs Ltd., Oxford, England) and a VAX 8650 computer (Digital Equipment Corporation, Maynard, Mass.).

HPLC analyses were carried out with an Altex Model 110A pump (Berkeley, Calif.) connected to a LKB 2140 Rapid Spectral Detector (Bromma, Sweden). The analytical

¹ Department of Medicinal Chemistry, School of Pharmacy, Virginia Commonwealth University, Richmond, Virginia 23298-0581.

² To whom correspondence should be addressed.

³ Chemistry Department, Randolph-Macon College, Ashland, Virginia 23005.

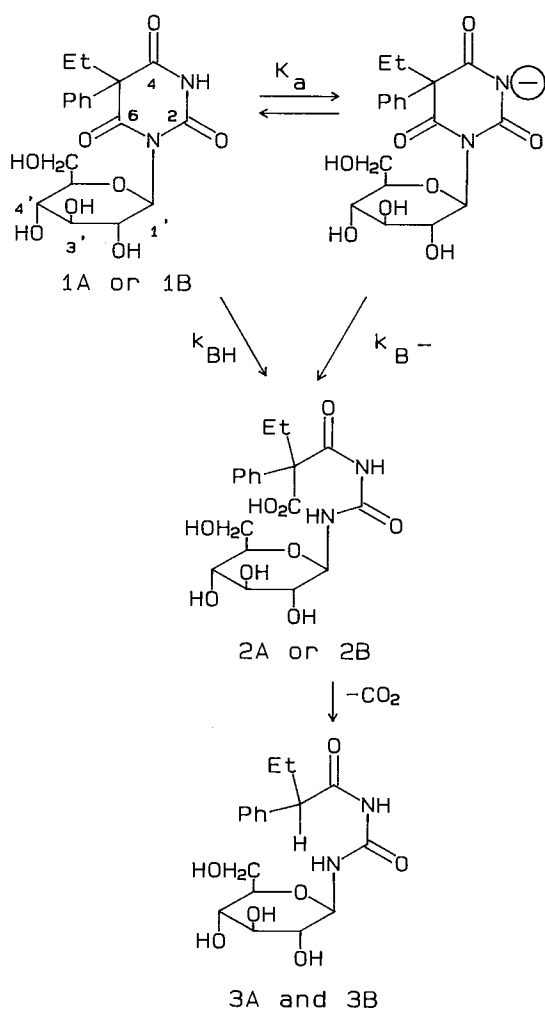


Fig. 1. Initial decomposition pathways for 1A and 1B at pH 7.4 and 37°C.

column used was an Alltech Econosphere, 5- μ m, C-18 reverse-phase column, 250 \times 4.6-mm i.d. (Deerfield, IL.). An ISCO V⁴ (Lincoln, Neb.) absorbance detector set at 254 nm was used for monitoring the HPLC separation during semipreparative purifications. The semipreparative column used was an Alltech Econosil, 10- μ m C-18 reverse-phase column, 250 \times 10-mm i.d.

The following are the experimental conditions for the thermospray LC/MS. The HPLC system was a Hewlett-Packard HP1090 liquid chromatograph (Avondale, Pa.) with a 20- μ l injection loop. The separation was achieved using the analytical HPLC column with a mobile phase of acetonitrile:0.1 M ammonium acetate buffer (30:70, v:v). The mass spectrometer was an HP 5988A LC/MS system interfaced to the HPLC using an HP thermospray interface. The interface was operated at a constant tip temperature (optimized) at 128°C with a 1.5 ml/min flow from the HPLC. For linear scanning the mass spectrometer scanned between m/z 100 and m/z 800 using 32 samples and an integration time of 100 μ sec. The signal was generated using the positive-ion, filament-on mode, with 1050-eV ionization energy. The ion source was at 320°C and the detection threshold was at 20000 counts.

Buffers and Stock Solutions

For the kinetic analysis, 0.105 M sodium phosphate buffers at pH 12.02, 11.04, 9.95, 9.04, 8.01, 7.00, and 6.06 were prepared at room temperature containing the appropriate amount of NaCl to maintain ionic strength at $\mu=0.7$. Addition of the stock solutions containing 1A or 1B gave a final 0.100 M phosphate buffer. The sodium borate buffer (pH 10.00) used for formation of the chromophore at 240 nm was prepared according to the method of Clark and Chan (10), except that it was 0.1 M.

Stock solutions were prepared by accurately weighing 1A (20.5 mg, 49.6 μ mol) or 1B (19.9 mg, 48.3 μ mol) into 1.00-ml volumetric flasks followed by dissolution and dilution to volume with 0.005 M H₃PO₄. These stock solutions were stored frozen.

METHODS

Separation and Purification of the Decomposition Products of Phenobarbital *N*-Glucosides

Compound 1A or 1B was dissolved in 500 μ l of 0.100 M sodium phosphate buffer at pH 7.4. The solution was placed in a screw-cap test tube with a Teflon-lined cap and maintained at 37°C. After 72 hr the reaction was slowed by freezing. The reaction mixture was purified by injection of 100- μ l aliquots onto the semipreparative column and separation was achieved using a mobile phase of acetonitrile:water (30:70, v:v) at a flow rate of 4.0 ml/min. Peaks were observed at 2.5, 3.8 (1A or 1B), and 7.6 min. Fractions were collected for retention volumes of 8.0–10.5 ml (fraction 2), 10.5–16.0 ml (fraction 1), and 26.5–32.0 ml (fraction 3). Samples were lyophilized for further analysis. Insufficient sample was available for elemental analysis.

Samples for thermospray LC/MS were prepared by heating 2 ml of a 150 μ M solution of 1A or 1B in 0.1 M ammonium acetate at 50°C for 1 hr in a heating block. The sample was then refrigerated until analyzed.

pK_a Determination

The pK_a's of 1A and 1B were determined spectrophotometrically (11). Solutions of 1A (2.48 μ mol) or 1B (2.42 μ mol) were prepared in 0.005 M H₃PO₄. A 100- μ l aliquot of this solution was mixed in a 1-ml quartz cuvette with 900 μ l of the appropriate 0.111 M sodium phosphate buffer (pH 6.50, 6.90, 7.00, 7.30, 7.50, 7.83, and 10.00) containing 0.5 M NaCl ($\mu=0.6$ –0.8). The absorbance at 240 nm was determined by the addition of 900 μ l of sodium borate buffer and the reading was recorded 3.0 min after mixing. The analysis was carried out in triplicate at each pH. For measurement of the unionized compound, 0.111 M H₃PO₄, pH 1.38, was used.

Kinetic Assay

The kinetic assays were carried out in a Teflon-lined screw-cap test tube in a heating block at the appropriate temperature. The reaction was initiated by adding 100 μ l of the 1A (4.96 μ mol) or 1B (4.83 μ mol) stock solutions to 1900 μ l of the temperature-equilibrated sodium phosphate buffer of the appropriate pH. The reaction mixtures were maintained at selected temperatures between 37 and 92°C. Ali-

quots (100 μ l) were withdrawn at suitable time intervals and diluted with sodium borate buffer (room temperature). The absorbance at 240 nm, referenced to the appropriate blank, was recorded immediately.

Molecular Modeling

Conformational analysis of 1A and 1B was performed by systematic rotation about the C_1-N_1 ($\tau_R = \tau_{C_2'C_1'N_1C_2}$, $\tau_H = \tau_{C_1'C_2'O_2'H}$) bond, optimizing all other geometrical parameters (bond length, bond angles, torsion angles) and minimizing molecular mechanics energy (MME within the CHEM-X system) at each step. The sign of the torsion angles is based on displacement of the last listed atom in a clockwise (+) or counterclockwise (-) direction relative to the bond defined by the first two atoms. Semiempirical molecular orbital calculations were performed using the AM1 method within AMPAC (QCPE 506, 12).

RESULTS

Identification of Decomposition Products

The decomposition of 20 mg (49 μ mol) of 1A resulted in the following lyophilized fractions, all as white powders: fraction 2A, 1.5 mg (2A); fraction 1A, 2.3 mg (1A); and fraction 3A, 12.0 mg (3A and 3B). The corresponding fractions starting with 30 mg (73 μ mol) of 1B: fraction 2B, 4.6 mg (2B); fraction 1B, 5.6 mg (1B); and fraction 3B, 18.7 mg (3A and 3B). Fractions containing 1A and 1B were identified as starting material based on identical HPLC retention times, UV spectra, and IR spectra compared to standards. Fractions containing 2A, 2B, 3A, and 3B were characterized as follows.

1-(1- β -D-Glucopyranosyl)-3-(2-ethyl-2-phenylmalonyl)urea (2A). $^1\text{H-NMR}$ (D_2O) δ 0.98 (t, $J=7.3$ CH₃, 3H), 2.40 (q, $J=7.3$, CH₂, 2H), 3.5 (br.d., CH₂-6'), 3.7–4.1 (br.m., H-2', H-3', H-4', H-5', 6H from 3.3 to 4.1), 4.9 (br.d., $J=12.9$, H-1', 1H), 7.43 (s, 5H). MS (m/z , %) 369 (100, M-CO₂ + H)⁺, 386 (91, M-CO₂ + NH₄⁺). When analyzed using the analytical HPLC column with a mobile phase of acetonitrile: 0.025 M sodium phosphate buffer, pH 6.5 (12:88, v:v), at a flow rate of 1.4 ml/min, detection at 198 nm; 2A, r.t. = 1.9 min (solvent front: r.t. = 16.5 min for 1A; r.t. = 18.5 for 1B; r.t. = 30.4 for phenobarbital).

1-(1- β -D-Glucopyranosyl)-3-(2-ethyl-2-phenylmalonyl)urea (2B). $^1\text{H-NMR}$ (D_2O) δ 0.99 (t, $J=7.1$, CH₃, 3H), 2.35 (br.m., CH₂, 2H), 3.53 (br.s., CH₂-6', 2H), 3.5–4.1 (br.m., H-2', H-3', H-4', H-5', 4H), 5.0 (br.m., H-1', 1H), 7.44 (s, 5H). MS (m/z , %) 369 (100, M-CO₂ + H⁺), 386 (91, M-CO₂ + NH₄⁺). Analysis by HPLC: 2B elutes in the solvent front when using the same mobile phase as described for 2A.

1-(1- β -D-Glucopyranosyl)-3-(2-phenylbutyryl)urea (3A and 3B). M.P. 114–117°C. From 1A a 67% yield; from 1B a 70% yield. $^1\text{H-NMR}$ (D_2O) δ 0.89 (dd, $J_{\gamma\beta}=7.4$, $J_{\gamma\beta'}=8.6$ Hz, CH₃, 3H), 1.88, 2.03 (m, $J_{\beta\beta'}=16.1$, CH₂, 2H), 3.4–3.6 (br.d., CH₂-6') 3.61 (t, $J_{\alpha\beta}=9.5$, $J_{\alpha\beta'}=7.8$), 3.7–4.0 (br.m., H-2', H-3', H-4', H-5', 7H from 3.4–4.0), 4.91 (br.d., $J=8.1$, H-1', 1H), 7.43 (s, 5H). IR (KBr): 3397.9, 3292.9, 1693.7, 1545.5, 1489.9, 1082.4, 1039.2, and 699.6 cm^{-1} . $[\alpha]_D^{24} = 0.76^0$ (c 3.3 mg/ml, methanol). MS (m/z , %) 369 (100, M + H⁺), 386 (34, M + NH₄⁺); λ_{max} 230 nm (ϵ 9.8×10^3) in

1.0 M NaOH. HPLC r.t. = 43.9 and 46.9 min using the same mobile phase described for 2A.

(2-phenylbutyryl)urea (PBU). The (2-phenylbutyryl)urea was prepared by decomposition of phenobarbital (12), m.p. 147.5–149°C (lit. 148–149°C). $^1\text{H-NMR}$ (CDCl_3) δ 0.87 (dd, $J_{\gamma\beta}=5.8$, $J_{\gamma\beta'}=8.6$ Hz, CH₃, 3H), 1.89, 2.01 (m, $J_{\beta\beta'}=20.7$, CH₂, 2H), 3.37 (t, $J_{\alpha\beta}=8.4$, $J_{\alpha\beta'}=7.1$, 1H), 7.30 (s, 5H). IR (KBr): 3397.9, 3342.3, 1681.3, 1391.1, 1175.7, 1094.7, and 699.6 cm^{-1} . λ_{max} 230 nm (ϵ 3.19×10^3) in 1.0 M NaOH. HPLC r.t. greater than 90 min using the same mobile phase as described for 2A.

The decomposition pathway consistent with the above compounds is depicted in Fig. 1.

pK_a Determinations

The pK_a's obtained for 1A and 1B are 7.06 (± 0.04) and 7.08 (± 0.05), respectively. The pK_a determined for phenobarbital under the same conditions is 7.18 (± 0.06). The pK_a of phenobarbital is in agreement with previous literature (14).

Kinetic Assay

The pseudo-first-order rate constants, k_{obs} , were calculated using the method of Duggleby (15) with a minimum of five data points. Correlation coefficients (r^2) of 0.98 or greater were obtained for each k_{obs} value that was calculated. A small residual absorbance, A_{∞} , was observed at all pH's below 11. When the decomposition was carried out in buffers from pH 8 to pH 10, significant residual absorbances which changed with time were observed after 7 to 10 half-lives. This anomalous behavior meant that a value for A_{∞} could not be determined directly. It appeared that additional reactions between one or more of the ring-opened hydrolysis products were occurring to produce new chromophores. This had previously been observed for the structurally similar 1,5,5-trisubstituted barbiturate, metharbital, when it was undergoing decomposition in phosphate buffers near pH 7 (16). As a result, absorbances measured to the point where the decrease in absorbance began to level off were used in the calculations. The inflection point was the initial estimate used as A_{∞} . Data points collected over a minimum of seven half-lives were fitted to the first-order rate law with iterative calculations of A_{∞} (15).

The pH-rate profiles for the decomposition of 1A and 1B are shown in Fig. 2. The two profiles show a section with a slope of approximately 1 at the highest concentration of hydroxide ion and a section of pH-independent decomposition in the pH range of the pK_a of the *N*-glucosides. This is expected for the alkaline hydrolysis of a weak acid in which the second-order rate constant is larger for the acidic (HB) than for the basic (B⁻) form. The sigmoidal shape of each curve is most consistent with a hydroxide ion-catalyzed degradation of the nonionized and ionized 1A and 1B. The k_{obs} at a given pH can be defined as

$$k_{\text{obs}} = k_{\text{BH}}[\text{OH}^-] \cdot f_{\text{BH}} + k_{\text{B}^-}[\text{OH}^-] \cdot f_{\text{B}^-} \quad (1)$$

where k_{BH} and k_{B^-} are the bimolecular rate constants for hydroxide ion attack on the undissociated (f_{BH}) and the ionized (f_{B^-}) forms of the barbiturate, respectively. Equation (1)

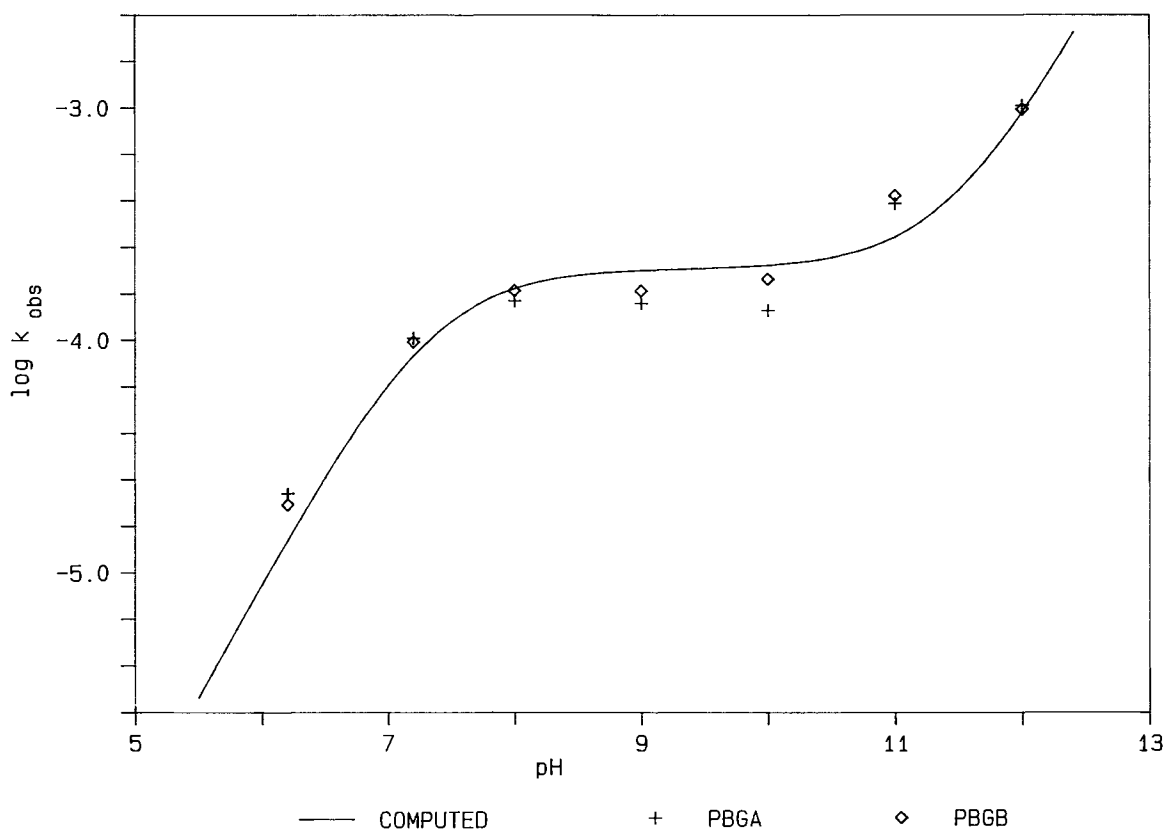


Fig. 2. pH-rate profile for decomposition of phenobarbital N-glucosides.

can be rewritten by substituting the terms of the equilibrium constant K_a for f_{BH} and f_{B^-} .

$$k_{\text{obs}} = \frac{k_{BH} \cdot K_w}{[H_3O^+]} \left[\frac{[H_3O^+]}{K_a + [H_3O^+]} \right] + \frac{k_{B^-} \cdot K_w}{[H_3O^+]} \left[\frac{K_a}{K_a + [H_3O^+]} \right] \quad (2)$$

The bimolecular rate constants that produced the best fits of the observed pH-rate profile with the measured pK_a values were calculated using the simplex algorithm of Nelder and Mead (17) as implemented in PCNONLIN (18). The values determined are given in Table I.

Dependence of Rate on Temperature

The Arrhenius parameters for the hydrolysis of 1A and 1B were calculated from the slopes and intercepts of plots of

the logarithm of the k_{obs} versus the reciprocal of the absolute temperature as outlined by Connors *et al.* (19). At pH 7.00, 8.01, 9.95, and 12.02, the reaction was carried out in the same buffer at two additional temperatures to obtain the thermodynamic data listed in Table II.

Molecular Modeling

Molecular mechanics calculations (MME within the CHEM-X system) were carried out to evaluate conformer populations that differ by rotation about the $C_1'-N_1$ bond. The diastereomer with the S configuration at the 5 position has two broad energy minima. At each minimum the barbiturate ring was approximately perpendicular to the glucose ring, with the 5 substituent oriented toward the β (syn) or α (anti) face of the glucose ring as depicted in Fig. 3. The energy minima occurred where τ_R ranges from -62 to -92° , i.e., when the barbiturate is in the anti region of the glucose

Table I. Catalytic Rate Constants for Some Barbiturates

	1A	1B	PB ^a	MB ^{a,b}
k_{BH}^c	861 (± 147)	1008 (± 154)	8.94	3.34
$k_{B^-} \times 10^{2c}$	8.0 (± 0.7)	7.2 (± 0.7)	0.35	27
Temperature	52	52	80	80
k_{obs} (37°C, pH 7.4) ^d	$(4.1 \pm 0.2) \times 10^{-5}$	$(3.4 \pm 0.1) \times 10^{-5}$	6.5×10^{-8}	—

^a Ref. 16.

^b Metharbital.

^c Liter \cdot mol⁻¹ \cdot sec⁻¹.

^d Sec⁻¹.

Table II. Apparent First-Order Rate Constants and Thermodynamic Parameters for the Decomposition of 1A and 1B

pH	Temp. (K)	E_{act} (kcal · mol ⁻¹)	k_{obs} (sec ⁻¹)	ΔH^\ddagger avg (kcal · mol ⁻¹)	ΔS^\ddagger avg (cal · mol ⁻¹ · K ⁻¹)
1A					
7.00	325.0	19.0	7.17×10^{-5}	18.3	-21.3
7.00	357.0		9.50×10^{-4}		
7.00	365.5		1.92×10^{-3}		
8.01	325.0	16.2	1.48×10^{-4}	15.6	-28.6
8.01	345.0		5.69×10^{-4}		
8.01	353.0		9.50×10^{-4}		
9.95	325.0	16.1	1.35×10^{-4}	15.5	-29.0
9.95	343.0		5.83×10^{-4}		
9.95	356.0		9.83×10^{-4}		
12.02	310.0	12.5	8.17×10^{-4}	11.9	-35.3
12.02	325.0		1.01×10^{-3}		
12.02	340.0		2.83×10^{-3}		
1B					
7.00	325.0	19.1	7.50×10^{-5}	18.4	-20.7
7.00	357.0		1.18×10^{-3}		
7.00	365.5		2.48×10^{-3}		
8.01	325.0	17.1	1.62×10^{-4}	16.4	-25.8
8.01	345.0		6.33×10^{-4}		
8.01	353.0		1.13×10^{-3}		
9.95	325.0	16.3	1.82×10^{-4}	15.6	-27.8
9.95	343.0		6.33×10^{-4}		
9.95	356.0		1.62×10^{-3}		
12.02	310.0	12.8	4.83×10^{-4}	12.1	-34.9
12.02	325.0		9.83×10^{-4}		
12.02	340.0		2.62×10^{-3}		

conformational space (S,anti), with calculated molecular mechanic energies between 12.4 and 12.8 kcal/mol. In this orientation, τ_{H} varied slightly, from -66 to -60° , with the C₂' hydroxyl proton-C₆ carbonyl oxygen distance varying from 3.36 to 2.52 Å. The conformer of slightly higher energy with $\tau_{\text{R}} = -92^\circ$, $\tau_{\text{H}} = -60$, and H···O of 2.52 Å approaches a conformation that allows hydrogen bonding between the glu-

ucose hydroxyl and the barbiturate carbonyl. The lowest-energy pathway for conversion of anti to syn conformers occurs via eclipsing of the N₁-C₂ bond of the barbiturate ring with the C₁'-C₂' bond of glucose with a barrier to rotation of 9 kcal/mol. In the syn region of conformational space (S,syn), a higher energy occurred with τ_{R} between 90 and 119° and τ_{H} between -59 and -58° . The energy calculated was between 13.8 and 13.4 kcal/mol, with the C₂' hydroxyl proton-to-C₂ carbonyl oxygen distance from 2.56 to 3.33 Å.

A similar distribution of conformers was observed for the diastereomer with the R configuration at the 5 position. Two broad minima occurred. A region of low-energy syn conformers (R,syn) was observed with τ_{R} between 91 and 119° , τ_{H} between -56 and -60° , and H···O between 2.48 and 3.32 Å, all with a molecular mechanics energy of 12.6 kcal/mol. The conversion of the syn conformer to the higher-energy anti conformer occurs via eclipsed N₁-C₁ and C₁'-C₂' bonds with a barrier to rotation of 6 kcal/mol. The anti conformer (R,anti) occurred within an energy range of 13.6 to 14.2 kcal/mol, τ_{R} of -61 to -87° , τ_{H} of -63 to -62° , and H···O from 3.38 to 2.62 Å.

Computational evaluation of the qualitative importance of hydrogen-bond formation to catalysis was carried out using the AM1 semiempirical quantum mechanical model (20). To evaluate the potential importance of hydrogen bonding of the C₂' hydroxyl to catalysis, models of both a hydrogen-bonded and non-hydrogen-bonded C₂ carbonyl and the hydrogen-bonded and nonhydrogen-bonded tetrahedral intermediate (addition of hydroxide ion) of the C₂ carbonyl were constructed, and relative calculated heats of formation compared. Hydrogen-bonding starting geometry was identical to

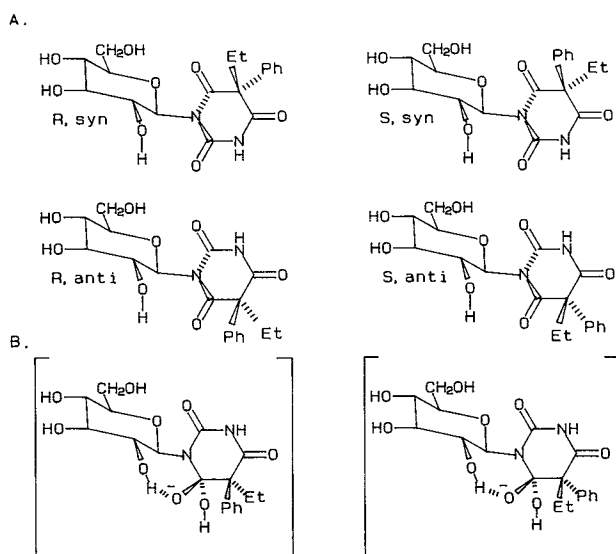


Fig. 3. (A) The anti and syn orientation of phenobarbital to glucose. (B) Intramolecular hydrogen bonding of C₂' hydroxyl, and the hydrated C₆ carbonyl of the tetrahedral intermediates.

that of the lowest-energy conformer of the R diastereomer with $\tau_R = 91^\circ$; however, τ_H was set to -27° . In this hydrogen-bonded structure the proton of the C_2' hydroxyl group pointed toward the C_2 carbonyl oxygen, with interatomic distance $H \cdots O = 2.1 \text{ \AA}$. A non-hydrogen-bonded structure with $\tau_H = 153^\circ$ was constructed and the heat of formation of both structures was calculated with AM1 without geometry optimization. The difference between the heat of formation of the hydrogen-bonded and that of the non-hydrogen-bonded structures is -1.7 kcal/mol . The heat of formation for intramolecular hydrogen bonding to the anionic oxygen of the tetrahedral intermediate was estimated in a similar fashion. Formation of the tetrahedral adduct reduces the $H \cdots O$ distance from 2.1 to 1.6 \AA . The heat of hydrogen-bond formation is -10.3 kcal/mol .

DISCUSSION

Hydrolytic degradation of medicinal barbiturates is well documented and has been extensively studied (16) and recently reviewed (21). The products of hydrolytic ring opening and possible pathways for their formation have been shown to be dependent on reaction conditions, such as temperature and pH, and structure. In general, the major initial degradation pathway for 5,5-di- and 1,5,5-trisubstituted barbiturates in aqueous solutions involves 1-6 or 3-4 ring opening and decarboxylation to give the 2,2-disubstituted acetylurea. An alternative minor pathway is 1-2 ring opening to give the 2,2-disubstituted diamide of malonic acid.

Based on mass spectra and proton NMR the compounds in fractions 3A and 3B were identified as *N*-glucose conjugates of PBU (Fig. 1). In the NMR the side-chain methylene appears as a complex multiplet associated with the diastereotopic methine proton present after decarboxylation. A

comparison of the proton spectra of PBU and the mixture of 3A and 3B is shown in Fig. 4. It is proposed that glucose is linked to the terminal urea nitrogen based on UV and proton NMR. The λ_{max} at 230 nm in 1 *N* NaOH for both 3A and 3B is identical to that of PBU, and a comparable ϵ is consistent with an ionizable imide. Consistent with N1 substitution of glucose is the appearance of the anomeric proton as a single doublet (9,23,24). The decomposition products in fraction 3A generated from 1A or in fraction 3B generated from 1B elute as two peaks with retention times longer than that of phenobarbital. Based on the peak area both decomposition products are present at a 1:1 ratio, therefore, racemization at C_5 has occurred during decarboxylation (22). Based on these spectroscopic observations, the compounds isolated from fractions 3A and 3B are identified as a 1:1 mixture of 1-(1- β -D-glucopyranosyl)-3-(2-phenylbutyryl)urea diastereomers. Therefore, 1A and 1B undergo 1-6 ring opening to give (2-phenylbutyryl)urea derivatives as the major product under conditions closely related to physiological conditions, i.e., neutral pH and 37°C.

The compounds in fractions 2A and 2B are identified as 1-(1- β -D-glucopyranosyl)-3-(2-ethyl-2-phenylmalonyl)urea. These compounds were initially identified as *N*-(1- β -D-glucopyranosyl)-2-ethyl-2-phenylmalonamide based on the mass spectrum, HPLC retention time, and chemical shift and coupling pattern ($^1\text{H-NMR}$) associated with aglycon portion of 2A and 2B. In the NMR the side-chain methylene appeared as a quartet which would be consistent with PEM coupled to glucose and PEM had been previously identified as a decomposition product from phenobarbital (21). Following isolation of 2A, the NMR indicated that it was approximately 50% contaminated with a PBU-related material based on the methylene and methyl

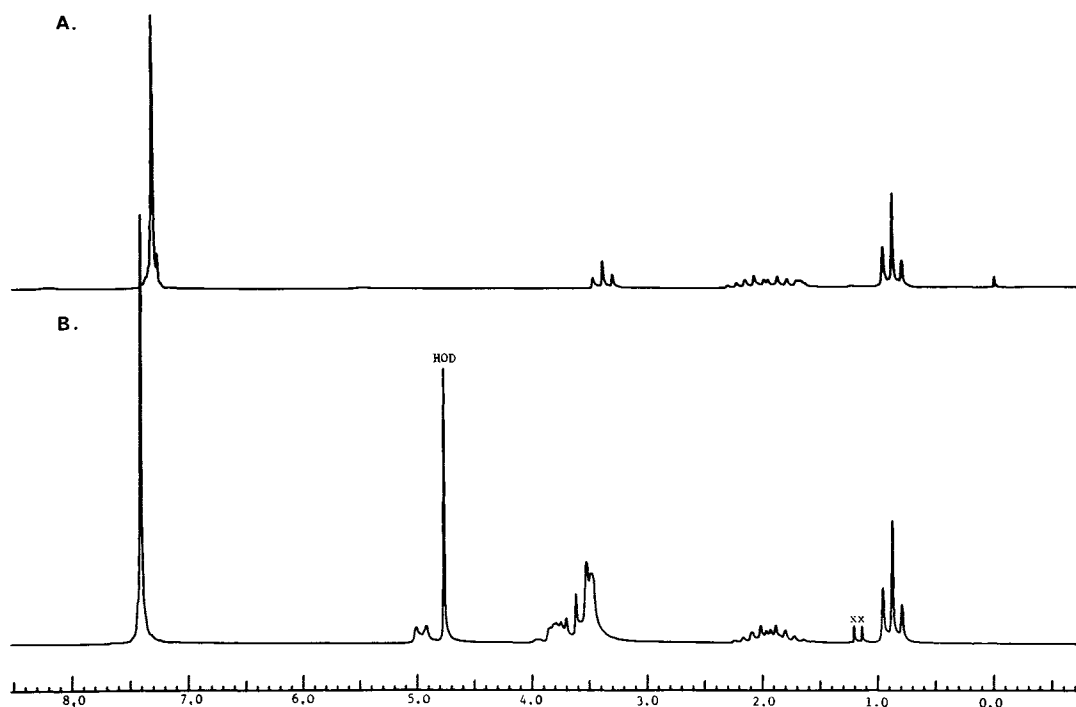


Fig. 4. $^1\text{H-NMR}$ of (A) (2-phenylbutyryl)urea in CDCl_3 and (B) both diastereomers of 1-(1- β -D-glucopyranosyl)-3-(2-phenylbutyryl)urea (3A and 3B) in D_2O .

resonances. Also, trace quantities of a related material could be observed in the NMR of 2B. Approximately 7 months later there was occasion to reanalyze these samples. Based on identification using $^1\text{H-NMR}$ and HPLC retention times, both 3A and 3B were obtained at a 2.4:1 ratio from the 2A sample and at a 1.3:1 ratio from the 2B sample. Therefore, the correct structures for 2A and 2B are 1-(1- β -D-glucopyranosyl)-3-(2-ethyl-2-phenylmalonyl)urea. No evidence for 1-2 or 2-3 ring opening to give an *N*-glucoside of phenylethylmalonamide was observed.

Phenobarbital was never observed as a decomposition product during any of these studies. Based on these observations the initial decomposition pathway proposed for both 1A and 1B is shown in Fig. 1.

Previous kinetic studies (21) with other barbiturates have shown that undissociated and monoanionic barbiturates hydrolyze with different pseudo-order rates at constant pH. The sigmoidal pH-rate profiles have been interpreted to indicate that degradation takes place by hydroxide ion attack on the undissociated and monoanion species. It is proposed here that the pH-rate profile of degradation of the phenobarbital *N*-glucosides is also due to differing rates of hydroxide ion attack on the nonionized and ionized species. An alternative mechanism (21) is that hydrolysis proceeds through two different pathways, in which the nonionized form of the barbiturate hydrolyzes via 1,2- or 2,3-ring opening to yield the substituted diamide, while the ionized form of the barbiturate hydrolyzes via 1,6-ring opening to yield the substituted acetyl urea product. In this study the amount formed of the glucose substituted (2-phenylbutyl)urea was determined at close to neutral pH. If the second possible mechanism occurs, the diamide product should be detectable and none was observed.

The Arrhenius parameters obtained for the hydrolysis of 1A and 1B are comparable to those reported for other barbiturates and consistent with the proposed mechanism. In particular, the entropies of activation (Table II) are large and negative at each pH evaluated (25), which is consistent with a bimolecular reaction. Within the pH range studied, a significantly (26) smaller negative ΔS^\ddagger is obtained at pH 7 than pH 12. From Eq. (2) and the experimentally determined values of K_a , k_{BH} , and k_{B^-} at pH 7, it can be shown that nearly all (99.996%) of the hydrolysis is due to hydroxide ion attack on the unionized barbiturate glucoside. Thus, the observed total entropy of activation (-21 eu) reflects decomposition via this pathway and is comparable in magnitude to base-catalyzed hydrolysis of urea (-20 eu) (27). At pH 12, 82% of the decomposition occurs by hydroxide ion attack on the ionized barbiturate glucoside and a larger total negative entropy of activation (-35 eu) is observed. The larger negative entropy of activation at alkaline pH is consistent with a bimolecular collision of two anions as required by the proposed mechanism (28,29).

The decomposition characteristics of the phenobarbital *N*-glucosides have closely paralleled what has been previously observed for the hydrolysis of barbiturates in general. As shown in Table I, when comparing the catalytic rate constants for hydrolysis of the *N*-glucosides to the 5,5-disubstituted barbiturates (phenobarbital) or 1,5,5-trisubstituted barbiturates (metharbital), the k_{B^-} or the rate

of hydrolysis of ionized species is of comparable magnitude to what has been previously observed (16). However, when comparing the k_{BH} or rate of hydrolysis of the nonionized species, the catalytic rate constant for hydrolysis of the *N*-glucosides at 54°C is more than two orders of magnitude faster than that of the comparably substituted metharbital at 80°C.

The differences in $\text{p}K_a$ values between phenobarbital and its glucoside conjugates do not account for the greater susceptibility of the conjugates to hydrolysis at neutral pH. It should be noted that although 1A and 1B are diastereomers and may exhibit different chemical reactivities, no significant differences were observed for the rates of hydrolysis of these compounds.

There are two plausible explanations for the increase in rate of the nonionized species. First, since the C_2' hydroxyl is in close proximity to the C_6 carbonyl, hydrogen bonding through a seven-member ring (30) could be proposed. This would polarize the carbonyl in the ground state, increasing the electrophilic character of the carbonyl carbon and making it more susceptible to hydroxide ion attack. Ground-state hydrogen-bond formation has been proposed to explain the rate enhancements observed for solvolysis of polysaccharides, steroids, and other natural products which contain a free hydroxyl in close proximity to an ester and is referred to as the Henbest-Kupchan effect (31-34). An alternative explanation of the Henbest-Kupchan effect involves a hydrogen bond to the tetrahedral hydrated carbonyl in the transition state rather than the carbonyl in the ground state (35).

The molecular modeling studies were carried out on the phenobarbital *N*-glucosides to determine the preferred conformation(s) and evaluate the importance of intramolecular hydrogen bonding in relation to the above theories. Conformational analysis clearly shows that both *N*-glucosides can accommodate a hydrogen bond between the C_2' hydroxyl group and the C_6 carbonyl oxygen. The intramolecularly hydrogen-bonded tetrahedral adduct was more stable than the non-hydrogen-bonded adduct by 10.3 kcal/mol. More importantly, the calculated hydrogen bond energy is 8.6 kcal/mol greater for the tetrahedral intermediate than for the ground-state carbonyl. These results suggest that a favorable intramolecular hydrogen-bond interaction may play a role in catalysis and lend further support to the mechanism proposed by Bruice and Fife (35) to explain the Henbest-Kupchan effect, i.e., hydrogen bonding contributes to catalysis by stabilizing the transition state rather than destabilizing the ground state.

Although hydrogen bonding facilitates hydrolysis, rate acceleration is normally only 10-fold over comparable structures that cannot hydrogen bond (35). The additional rate enhancement is probably due to hindered rotation around the glycosidic bond and the aglycon, which is nearly equivalent to the elimination of one rotational degree of freedom in the ground state. Therefore, the 100 fold rate acceleration observed for 1A and 1B may be attributable to hydrogen-bond formation in an entropically favorable fashion.

In principle, intramolecular catalysis of hydrolysis should be observed for other *N*-glycosylated imides. Consistent with this concept is the facile alkaline hydrolysis of the hydantoin ring of phenylethylhydantoin *N*-glucuronide.

It was proposed that the ring hydrolysis was catalyzed by the glucuronic acid moiety, although no mechanistic studies were carried out (37).

Finally, these studies require the reevaluation of any data related to phenobarbital *N*-glucosides (3–8) in relation to the quantitative importance of the *N*-glucosylation pathway. The validity of any previous study will be dependent on the pH of the urine and the conditions under which the samples have been collected, stored, and analyzed. In our own studies prior to observing this problem (6–8), no effort was made to control for decomposition, even though samples were refrigerated immediately following collection and frozen within 48 hr. In one individual who had taken a 90-mg peroral dose of phenobarbital at two different times, the percentage of the dose of phenobarbital excreted in the urine over 150 hr as phenobarbital *N*-glucosides was 3.4% when collected using the normal procedure, versus 12.4% when the urine was acidified immediately with citric acid (data not included). It is recommended that urine collected for analysis of the *N*-glucosides of phenobarbital be acidified immediately; citric acid was found to be an effective acidifying agent in studies currently in progress. In addition to decomposition after collection, significant decomposition of the *N*-glucoside could occur in the plasma and/or neutral to basic urine, since the half-life of these compounds is approximately 5.0 hr at pH 7.4 and 37°C. The pharmacology/toxicology and metabolism associated with these decomposition products are unknown. Finally, the importance of this decomposition in relation to the quantitative studies on the urinary excretion of the *N*-glucosides of amobarbital and whether these compounds are equally susceptible to hydrolysis are unknown.

In conclusion, the initial observation that the *N*-glucosides of phenobarbital were unstable at pH 6.5 prior to analysis when sitting in an HPLC autoinjector has led to studies which have provided a better understanding of the chemistry associated with these novel metabolites. These observations may contribute to a better understanding of the biodisposition associated with phenobarbital and other structurally related drugs.

ACKNOWLEDGMENT

This work was supported by PHS Grant GM34507.

REFERENCES

1. B. K. Tang, W. Kalow, and A. A. Grey. *Res. Commun. Chem. Pathol. Pharmacol.* 21:45–53 (1978).
2. W. H. Soine, P. J. Soine, B. W. Overton, and L. K. Garrettson. *Drug Metab. Disp.* 14:619–621 (1986).
3. B. K. Tang, W. Kalow, and A. A. Grey. *Drug Metab. Disp.* 7:315–318 (1979).
4. D. Kadar, B. K. Tang, and A. W. Conn. *Can. Anaesth. Soc. J.* 29:16–23 (1982).
5. B. K. Tang, B. Yilmaz, and W. Kalow. *Biomed. Mass Spectrom.* 11:462–465 (1984).
6. W. H. Soine, V. O. Bhargava, and L. K. Garrettson. *Drug Metab. Disp.* 12:792–794 (1984).
7. V. O. Bhargava, W. H. Soine, and L. K. Garrettson. *J. Chromatogr.* 343:219–223 (1985).
8. V. J. Bhargava and L. K. Garrettson. *Dev. Pharm. Ther.* 11:8–13 (1988).
9. W. H. Soine, P. J. Soine, T. M. England, B. W. Overton, and S. Merat. *Carbohydr. Res.* (submitted for publication).
10. C. R. Clark and J. Chan. *Anal. Chem.* 50:635–637 (1978).
11. A. Albert and E. P. Serjeant. *The Determination of Ionization Constants, A Laboratory Manual*, 3rd ed., Chapman and Hall, New York, 1971, pp. 70–101.
12. J. J. P. Stewart. *QCPE Bull.* 6:24 (1986).
13. F. Fretwurst. *Arzneim. Forsch.* 8:44–50 (1958).
14. M. E. Krahl. *J. Phys. Chem.* 44:449–462 (1946).
15. R. G. Duggleby. *Anal. Biochem.* 110:9–18 (1981).
16. E. R. Garrett, J. T. Bojarski, and G. J. Yakatan. *J. Pharm. Sci.* 60:1145–1154 (1971).
17. J. S. Nelder and R. Mead. *Comput. J.* 7:308–313 (1965).
18. Statistical Consultants, Inc. *Am. Stat.* 40:52 (1986).
19. K. A. Connors, G. L. Amidon, and V. J. Stella. *Chemical Stability of Pharmaceuticals: A Handbook for Pharmacists*, 2nd ed., John Wiley and Sons, New York, 1986, pp. 8–62.
20. M. J. S. Dewar, E. G. Zoebisch, E. F. Healy, and J. J. P. Stewart. *J. Am. Chem. Soc.* 107:3902–3909 (1985).
21. J. T. Bojarski, J. L. Mokrosz, H. J. Barton, and M. H. Paluchowska. *Adv. Heterocycl. Chem.* 38:229–297 (1985).
22. E. L. Eliel. *Stereochemistry of Carbon Compounds*, McGraw-Hill, New York 1962, pp. 384–393.
23. J. C. Jochims, H. von Voithenberg, and G. Wegner. *Chem. Ber.* 111:2745–2756 (1978).
24. J. C. Jochims, H. von Voithenberg, and G. Wegner. *Chem. Ber.* 111:1693–1708 (1978).
25. P. J. Robinson. *J. Chem. Ed.* 55:509–510 (1978).
26. K. B. Wiberg. *Physical Organic Chemistry*, J. Wiley and Sons, New York, 1964, pp. 377–379.
27. K. R. Lynn. *J. Phys. Chem.* 69:687–689 (1965).
28. See Ref. 26, pp. 390–393.
29. E. F. Hammel, Jr., and S. Glasstone. *J. Am. Chem. Soc.* 76:3741–3745 (1954).
30. A. B. Foster, A. H. Haines, and M. Stacey. *Tetrahedron* 16:177–185 (1961).
31. S. M. Kupchan, S. P. Eriksen, and M. Friedman. *J. Am. Chem. Soc.* 88:343–346 (1966).
32. S. M. Kupchan, S. P. Eriksen, and Y.-T. S. Liang. *J. Am. Chem. Soc.* 88:347–350 (1966).
33. R. W. Wright and R. H. Marchessault. *Can. J. Chem.* 46:2567–2575 (1968).
34. H. B. Henbest and B. J. Lovell. *J. Chem. Soc.* 1965–1969 (1957).
35. T. C. Bruce and T. H. Fife. *J. Am. Chem. Soc.* 84:1973–1979 (1962).
36. G. Buemi, F. Zuccarello, and A. Randino. *J. Mol. Struct. (Theochem.)* 164:379–389 (1988).
37. J. H. Maguire, T. C. Butler, and K. H. Dudley. *Drug Metab. Disp.* 10:595–598 (1982).